nature physics

INSIGHT | REVIEW ARTICLE

https://doi.org/10.1038/s41567-021-01357-2

Quantum science with optical tweezer arrays of ultracold atoms and molecules

Adam M. Kaufman [1]✉ and Kang-Kuen Ni [2]✉

Single atoms and molecules can be trapped in tightly focused beams of light that form 'optical tweezers', affording exquisite capabilities for the control and detection of individual particles. This approach has progressed to creating tweezer arrays holding hundreds of atoms, resulting in a platform for controlling large many-particle quantum systems. Here we review this new approach to microscopic control of scalable atomic and molecular neutral quantum systems, its future prospects, and applications in quantum information processing, quantum simulation and metrology.

Over the past two decades, optical tweezer arrays of atoms and molecules have emerged as a powerful platform for the preparation and manipulation of ultracold neutral particles[1–10]. In such experiments, tunable arrays of individual particles are trapped under ultrahigh vacuum by shining a laser beam through a microscope objective, creating foci of light that trap individual atoms (Fig. 1).

The technique is built upon work in the early 2000s[1] that demonstrated that single atoms could be loaded into micrometre-scale optical potentials from a laser-cooled cloud of atoms, and read out with high-fidelity fluorescence microscopy via the same imaging system used to project the tweezers. As the trapping is based on control of precisely tunable optical fields, the system derives much of its power by translating optical engineering techniques into engineering of large-scale atomic arrays[11–15]. While isolated single atoms in an ordered array of separated potentials were previously realized through sophisticated phase transitions in optical lattice systems[16], now such conditions are reached with what have become basic laser-cooling and optical techniques.

With these methods, ordered, microkelvin conditions are achieved on subsecond timescales, enabling studies where fast statistics acquisition and experimental duty cycles are critical. This combination of microscopic control and detection, speed, and versatility has had wide-ranging use in quantum science, in fields ranging from quantum optics and quantum information[17–19], to many-body physics[6,20–24], metrology[25–27], nanophotonics[28–31] and ultracold collisions[8,32–35].

Pioneering work

In a series of experiments, it was shown that laser-cooled neutral atoms in a micrometre-scale focus of light (the optical tweezer) experience a 'collisional blockade', wherein atoms are ejected in pairs from the tweezer region through optically enhanced dipole–dipole interactions[1,36]. The collisional blockade (Box 1) process correspondingly converts a population of N atoms within the tweezer to the parity of N, yielding stochastic, sub-Poissonian loading of zero atoms or one atom (Fig. 1).

High-resolution microscope objectives can readily achieve a tweezer focus below one micrometre, creating a robust, millikelvin-scale deep trap with only milliwatts of optical power. Using this new single-atom source to create an ideal two-level system allowed for seminal experiments in quantum optics, including triggered single-photon sources and fundamental studies of Hong–Ou–Mandel interference of independently generated photons[17,18], as well as demonstrations of quantum state control of single neutral atoms in tweezers[37,38].

Rapid creation of low-entropy neutral-atom tweezer arrays

In spite of the versatility and simplicity of the tweezer platform, a clear shortcoming has been the higher entropy of atoms in tweezer arrays compared with, for instance, the entropy exhibited in an atomic Mott insulator[16] using conventional optical lattice methods. This entropy arises in two ways: first, the motional temperatures of the individual atoms, and second, the stochastic 50% density filling of the array from loading the tweezer with the collisional blockade process. The first form of entropy impacts quantum control schemes that benefit from or require pure ground-state preparation of each atom[19,39]. The second form of entropy is an impediment to scalability, for example, for use as a platform for quantum simulation and quantum computing, where deterministic preparation of defect-free arrays is highly desirable.

While not always required, mitigating both forms of entropy would allow tweezer-based assembly of degenerate systems from individual atoms[4,40]. Quantum degeneracy can be achieved with ultracold gases in optical lattices, but the tweezer platform would provide significantly enhanced cycle times and statistics acquisition.

The motional entropy in tweezers has primarily been tackled in two ways. First, in 2010, a set of experiments demonstrated that deterministic preparation of degenerate Fermi gases could be achieved by overlapping optical tweezers with evaporatively cooled clouds[41] rather than thermal laser-cooled clouds. The overlapped tweezers isolated the coldest atoms from the sample, realizing within the tweezer highly degenerate, idealized gases of spin-half fermions. Deterministic number preparation was achieved through clever spilling techniques, allowing full control of the spin and number distribution. This approach has been used to study the transition between few-body and many-body physics[42], fermionization[43], coherent tunnelling dynamics of fermions[44], entanglement and correlations[45–47], and other essential features of interacting fermions[48,49].

To retain the fast cycle times and reduce experimental complexity, it was also desirable to explore how to lower motional entropy after loading single atoms from a purely laser-cooled (thermal) cloud. In this case, the evaporative-cooling method is unavailable as this cooling relies on atomic collisions within samples of many atoms. In 2012, it was shown[50,51] that the confinement afforded by an optical tweezer was amenable to a technique known as 'sideband cooling' (Box 2) that had been developed in trapped-ion experiments[52,53]. This laser-cooling technique enables preparation of atoms in their

[1]JILA, NIST and Department of Physics, University of Colorado, Boulder, CO, USA. [2]Department of Chemistry and Chemical Biology, Harvard University, Cambridge, MA, USA. ✉e-mail: adam.kaufman@colorado.edu; ni@chemistry.harvard.edu

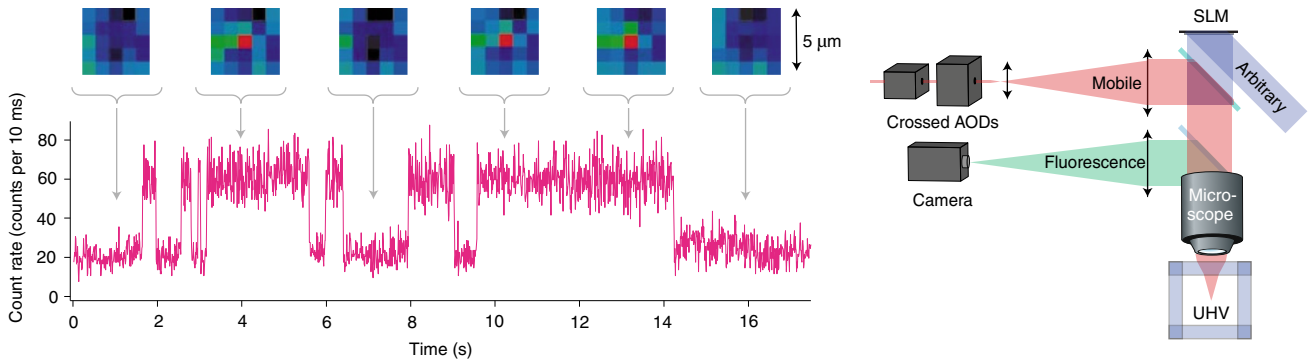

Fig. 1 | Neutral atoms in optical tweezers. Right: typical set-up and technology used in a neutral-atom optical tweezer trapping experiment. A spatial light modulator (SLM) and set of acousto-optic deflectors (AODs) are used to create arrays of tunable (blue) and rearrangeable (red) optical potentials, which are projected through a high-numerical-aperture objective (0.5 or above is typical) to trap single atoms under ultra-high vacuum (UHV). A high-sensitivity camera can be used to image single atoms in these potentials via their fluorescence (green). Left: an example sequence of images from ref. [1] is shown, illustrating the binarized presence or absence of atoms in a single tweezer trap through the fluorescence counts on the camera. Figure adapted with permission from ref. [1], Springer Nature Ltd.

three-dimensional motional ground state with a greater than 90% success rate in tens of milliseconds, which is between ten and a thousand times faster than evaporative-cooling schemes.

With single atoms cooled to the three-dimensional ground state of optical tweezers, it became possible to study single-band tunnelling physics of indistinguishable atoms in a pair of tweezers, allowing the first observation of the Hong–Ou–Mandel effect with atoms (Fig. 2b) as well as studies of spin-exchange-based entanglement of individually addressed atoms[4,39]. Precise control of atomic motion also allowed the groundbreaking demonstration of coupling a neutral atom to nanophotonic structures[28]. Holding an atom near the highly confined optical mode of a nanophotonic structure provides enhanced atom–photon interactions while requiring the suppression of thermal fluctuations to well below the spatial size of the optical mode. The combination of laser-cooled atoms in mobile tweezers and nanophotonic structures has continued to be an exciting direction since this first demonstration for novel atom–photon interfaces[29–31]. This cooling method may also prove valuable for high-fidelity Rydberg two-qubit gate schemes sensitive to Doppler effects as well as using tweezers to synthesize ultracold molecules[10,54,55].

A second critical set of advances improved the overall filling fraction in laser-cooled tweezer arrays to near unity. Here, defect-free conditions are realized by leveraging the tunability of the tweezer positions and depths to rearrange the atoms to fill empty tweezers[12,13]. This simple but powerful technique can be implemented in multiple ways. In one approach, after detecting the random distribution of atoms within a one-dimensional array, empty tweezers can be extinguished while the entire chain is spatially compressed to leave a homogeneously filled array of atoms (Fig. 2a, top). In another approach, a two-dimensional array is detected, and then atoms from the edge of the array may be transported with an auxiliary mobile tweezer to empty sites, yielding a central region of filled tweezers (Fig. 2a, bottom).

The use of acousto-optic deflectors and spatial light modulators—a versatile optical engineering technology—provides the real-time control necessary for the rearrangement and flexibility in the target atomic geometries. This method allows the creation of defect-free arrays of tweezer-trapped atomic qubits, a versatile tool for quantum computing and simulation, discussed below and in ref. [24]. This work has since been extended to three dimensions[56] for arrays of 72 atoms at 95% filling fraction and larger two-dimensional array sizes of 200 atoms and 99.2% filling[57,58]. To reach thousands of atoms, it is possible that rearrangement will be combined with enhanced loading schemes[59–61] (Box 1), as the rearrangement time scales extensively with the number of defects and the overall fidelity of the operations is fundamentally limited by the vacuum lifetime.

The ingredients discussed so far enable the creation of tens to hundreds of ultracold atoms in defect-free, tunable arrays with single-particle-resolved readout, an effective resource for quantum science. They establish the concept of assembly of ultracold matter, one atom at a time, a characteristic that has been critical to many advances in recent years. Furthermore, many of the basic mechanisms (light-assisted collisions and laser cooling) have also been exploited in tunable lattices[11,14] with great success, resulting most recently in defect-free three-dimensional arrays of ground-state cooled atoms[15].

Rydberg atoms in tweezers

Single neutral atoms in tweezers offer excellent coherence properties because the effects of atomic collisions on internal state coherence are largely eliminated, a key strength for some of the metrological work discussed in the next section. However, this strength comes at the cost that engineering interactions between the atoms—a requirement for generating and studying entangled quantum systems—must be enabled by introducing wavefunction overlap or through the creation of long-range interaction potentials. The former has been achieved using ground-state cooled atoms in tweezers[39], with the challenges that the interaction timescales can be slow and realizing the requisite wavefunction overlap is non-trivial. The latter approach of long-range interactions has been the focus of much work in the past decade, via so-called Rydberg interactions.

The concept of using Rydberg interactions to create two-qubit entanglement between tweezer-trapped atoms dates back to a seminal theory proposal[62] and the first demonstration of neutral-atom optical tweezer trapping[1]. The strategy suggested was simple: by optically exciting a pair of neutral atoms separated by a few micrometres to a 'Rydberg' excited state with a high principal quantum number, the resulting van der Waals dipole–dipole interactions could be harnessed for quantum information processing and many-body spin models[19,63] (Fig. 3a). The energy scale of these interactions reaches tens to hundreds of megahertz. This greatly exceeds the lifetimes of Rydberg states, which vary from tens of microseconds to tens of milliseconds depending on the Rydberg level that is determined by radiative decay and blackbody-induced transitions between Rydberg levels.

Box 1 | Collisional blockade

Collisional blockade is a mechanism that limits the number of atoms (or molecules) trapped in an optical tweezer to no more than one[36]. While initial loading might cool several atoms into an optical tweezer, subsequent light-assisted collisions then take place to eject particles in pairs, leaving behind either one atom or zero atoms trapped in the tweezer, each with roughly 50% probability. The physical mechanism of the pair-wise ejection can be understood using the following semiclassical picture, taking alkali atoms as an example[148]. For any homonuclear pair of atoms separated by distance R, their long-range potential varies as $\frac{-1}{R^6}$ to the electronic state S+S asymptote, while their long-range potential varies as $\frac{-1}{R^3}$ to the S+P asymptote. When an atom absorbs a photon (red straight arrow) from red-detuned laser cooling light, the two atoms on the $\frac{-1}{R^3}$ potential attract (black arrow) before a redder photon (red wavy arrow) is spontaneously emitted. The total energy gained by the atom pair is sufficient to eject both atoms out of the tweezer. Notably, it is also possible to modify the light-assisted collisions such that the stochastic loading is improved from ~50% up to a current record of 91% (ref. [59]). This is accomplished by detuning the laser that drives the light-assisted collisions to the blue, which bounds the energy imparted during a collision so that there is only enough energy for a single atom in the pair to be ejected rather than both[59]. This approach was subsequently adapted to two-by-two arrays with 91% filling[60] and improved on using grey-molasses-cooling techniques to ten-by-ten arrays at 80% filling fraction[61].

For heteronuclear collisions, the situation is different because the excited-state long-range potential is $\frac{-1}{R^6}$, which matches more similarly to the ground-state long-range potential, and it takes many more photon-scattering events to eject the atoms. For other species, such as alkaline-earth atoms and molecules, where the homonuclear pair situation applies, the general mechanism for light-assisted collisions hold. The differences are in the details. For alkaline-earth atoms, light-assisted collisions can be induced by applying near-resonant light with a broader cooling transition because the narrow-linewidth laser-cooling light would otherwise scatter photons too slowly[78,79], and for molecules, the underlying pair potentials are unknown[9].

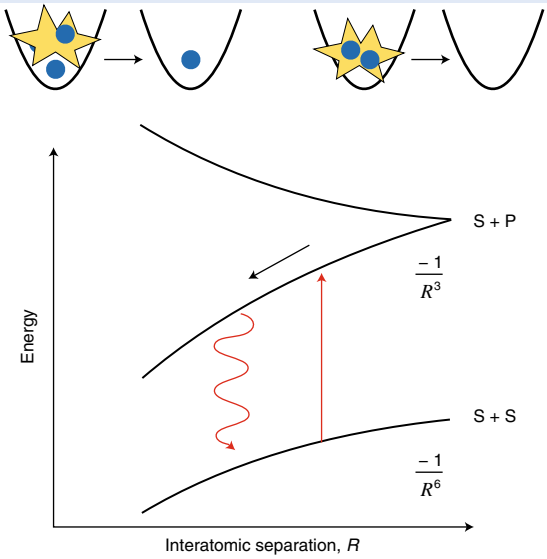

Importantly, the Rydberg interactions are optically switchable and can be spatially resolved with patterned light fields, representing a powerful tool for creating interacting many-body quantum systems with a variety of spin–spin interactions[6,20–23], as well as digital quantum circuit models. The former is the subject of a recent review article[24], and so, here, we focus on recent developments in quantum information with tweezer-trapped atoms using Rydberg-mediated gates.

Models of quantum information processing typically assume a set of experimental requirements that includes a qubit with long-lived coherence compared with relevant gate times, single-qubit control, single-qubit readout, and two- or multi-qubit gate interactions. A qubit encoded in hyperfine levels of tweezer-trapped alkali atoms exhibits long coherence times, allowing high-fidelity rotations through microwave or Raman spectroscopy and low qubit-to-qubit cross-talk within an array. Recent work using a two-dimensional tweezer array of caesium atoms demonstrated single-qubit addressing with fidelity exceeding 99% with cross-talk at the 10^{-3} level[5]. In parallel with the development of single-qubit capabilities, two-qubit gates based on Rydberg interactions have significantly advanced with time, beginning with early demonstrations of the Rydberg blockade effect[64,65] and then two-qubit gates[2,3]. These groundbreaking two-qubit gate experiments showed entanglement in long-lived (hyperfine) qubit states. Early work reported a Bell-state fidelity near 75%, limited by technical issues including trap loss, detection errors, laser phase coherence and temperature effects[2,3]. Building on these results, more robust gate schemes using optimized laser sweeps resulted in an enhanced two-qubit fidelity of 81% (ref. [66]). More recently, improved understanding and control of the lasers used for Rydberg excitation significantly increased the fidelity of the blockade interaction[7,67], on the heels of which came the most recent demonstrations of two-qubit gates with Bell-state fidelities of 97.4(3)% in globally addressed one-dimensional arrays and 88(2)% in a locally addressed two-dimensional array[68,69] (Fig. 3b,c). More advanced entanglement generation schemes can leverage the long-range interaction[70,71]—for example, the recently demonstrated three-qubit Toffoli gate[68] or 20-particle cat states[22] through many-body sweeps—to realize quantum algorithms in fewer steps.

With existing apparatuses, the control of high-fidelity transverse Ising spin models establishes the prospect of studying quantum-enhanced performance in near-term devices. There has been a particular focus on variational algorithms and natural encodings of Max-cut and sampling problems into Rydberg blockade models[72–74]. Further improvements to remove blackbody effects and reach the fundamental coherence time limit set by radiative decay will require tweezer array systems in a cryogenic environment. This could potentially lead to factor-of-ten-level improvements in gate fidelity[19,75]. Cryogenic trapping would be especially useful for exploiting the greatly enhanced radiative lifetimes—tens of milliseconds, corresponding to a thousand-fold improvement—of circular Rydberg states[19,76]. Meanwhile, multi-species experiments in the spirit of mixed species ion traps may be employed to improve the fidelities of local qubit measurement and explore new two-qubit gate schemes[75,77].

Alkaline-earth atoms in tweezers

As with early work in quantum gases, the pioneering studies in optical tweezer trapping of neutral atoms focused on alkali atoms, the single valence electron of which admits simple, robust laser cooling. In recent years, there has been growing interest in exploring the use of tweezer trapping for more complicated particles, where additional internal degrees of freedom might expand the scope of scientific applications. This interest is reflected in two major efforts over the past five years, including tweezer trapping of alkaline-earth atoms and of molecules. In this section we focus on emerging topics regarding the former, while in the next section we discuss the latter.

Beginning with the first demonstrations[78–80], the field of alkaline-earth atoms in tweezers has been moving quickly with a number of directions under investigation (Fig. 4). With two valence

Box 2 | Laser cooling single neutral atoms to the motional ground state

Once single atoms are loaded into individual tweezers, optical cooling may be used to cool the atoms to the motional ground state, following pioneering work with trapped ions[53] and later neutral atoms in optical lattices[149,150]. In the first step of cooling, a coherent transition occurs between $|\uparrow;n\rangle \rightarrow |\downarrow;n-1\rangle$ with a pair of Raman beams whose differential k-vector projects onto the motional axis quantized in n and is resonant with a transition that changes the atomic spin and removes a motional quantum of energy ($\hbar\omega$). Then, in a second step, optical pumping (OP) recycles the atom back to the initial spin state through an excited state ($|e\rangle$), where the spontaneously emitted photons carry away entropy. If the tweezer trap is sufficiently confining (that is, within the Lamb–Dicke regime), then the momentum imparted by the scattered optical pumping photon does not change the motional state of the atom, transferring the population from $|\downarrow;n-1\rangle$ to $|\uparrow;n-1\rangle$. The cooling process then repeats until the atom is in the motional ground state, at which time it decouples from both drives. This is accomplished with a set of beams (shown in **a**) that drive coherent transitions that change the motional state and internal state of the atom (Raman beams, 'RB' in the figure), as well as initialize the atom in a particular spin state through optical pumping (see the level diagram in **b**). By having several pairs of Raman beams that each couple to separate motional axes, this ground-state cooling process can be performed on all three dimensions of the tweezer. We also point out that this scheme can be adapted to forgo the need of separate Raman beams and optical pumping, by using optical transitions whose linewidth is less than the trap frequency[52]. Figure adapted with permission from ref. [50] under a Creative Commons licence CC BY 3.0.

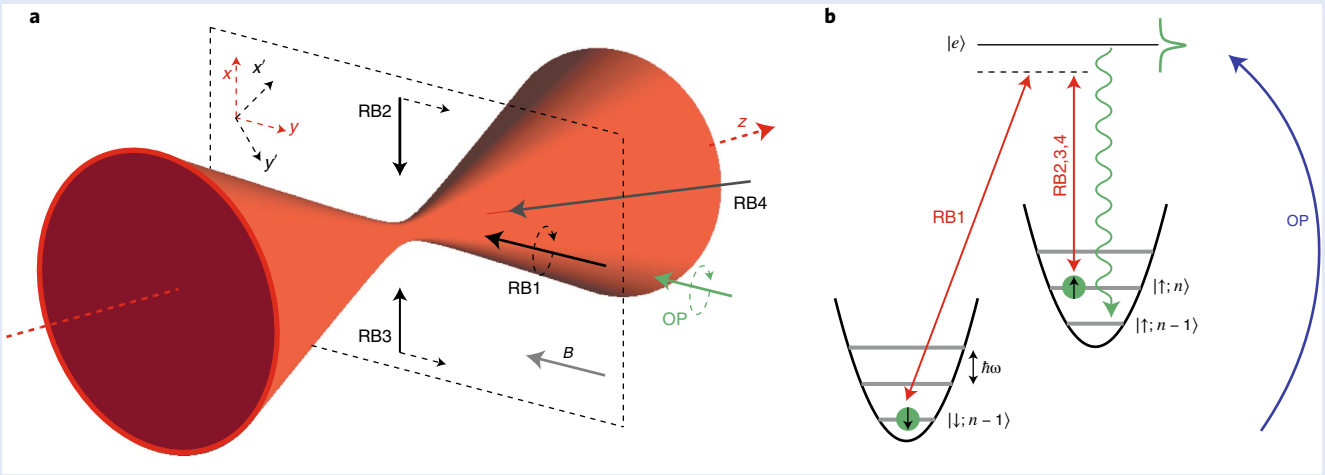

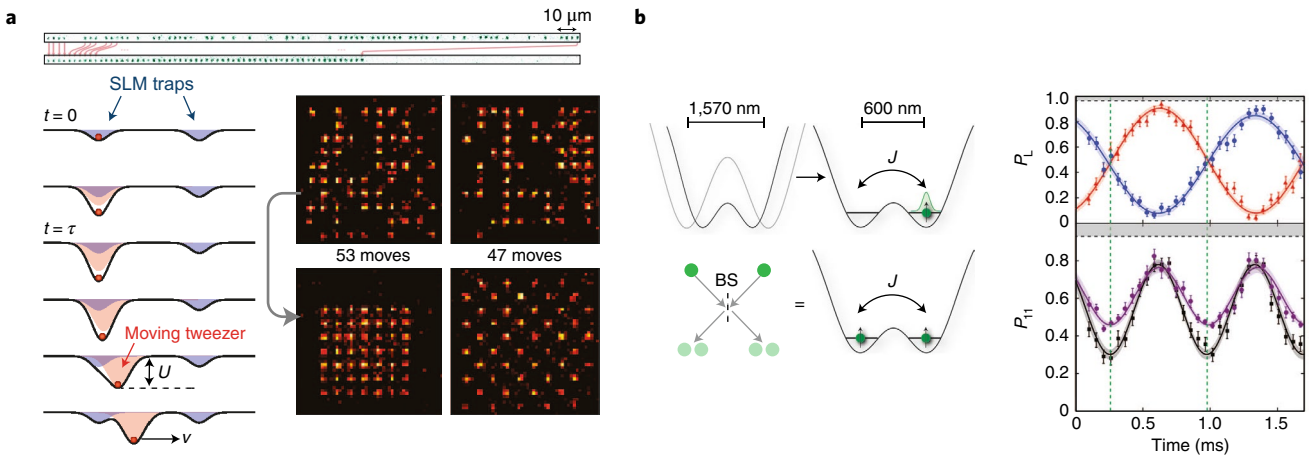

Fig. 2 | Entropy mitigation by rearrangement and ground-state cooling. a, Using the real-time tunability of the tweezer positions, the positions of trapped atoms can be moved around in one dimension (top) or two dimensions (bottom right), such that an initial array with empty sites can be rearranged to create a 'defect free' region. As an example, on the bottom left, a static, shallow potential made by an SLM can hold atoms, while they are dragged with a mobile tweezer into vacant sites. The method creates defect-free arrays, which are useful for the realization of many-body spin models of long-range interacting atoms. **b**, Removing motional entropy through ground-state cooling (Box 2) opens new directions. For instance, combining cooling with the tunability of the tweezer positions can create conditions where atoms can tunnel and undergo atomic beamsplitting interactions between tweezer sites. With adequate cooling, the atoms can be made indistinguishable, allowing the observation of the atomic Hong–Ou–Mandel effect[4]. The top plot shows the single-particle tunnelling dynamics of a single atom in a double well with coupling J, beginning in the left (right) well in blue (red) and the probability to end up in the left well (P_L); the bottom plot shows the two-particle dynamics in terms of the probability P_{11} for atoms to reside in separate wells, where the Hong–Ou–Mandel interference is manifest in the regions of the plot where the measured P_{11} falls below the expectation for P_{11} (dashed green lines) for distinguishable atoms (purple), indicating that the atoms are in a superposition of both being in the left well and both being in the right well. Error bars are the standard error in the measurement. Panels adapted with permission from: **a**, ref. [12], AAAS; ref. [13], AAAS; **b**, ref. [4], AAAS.

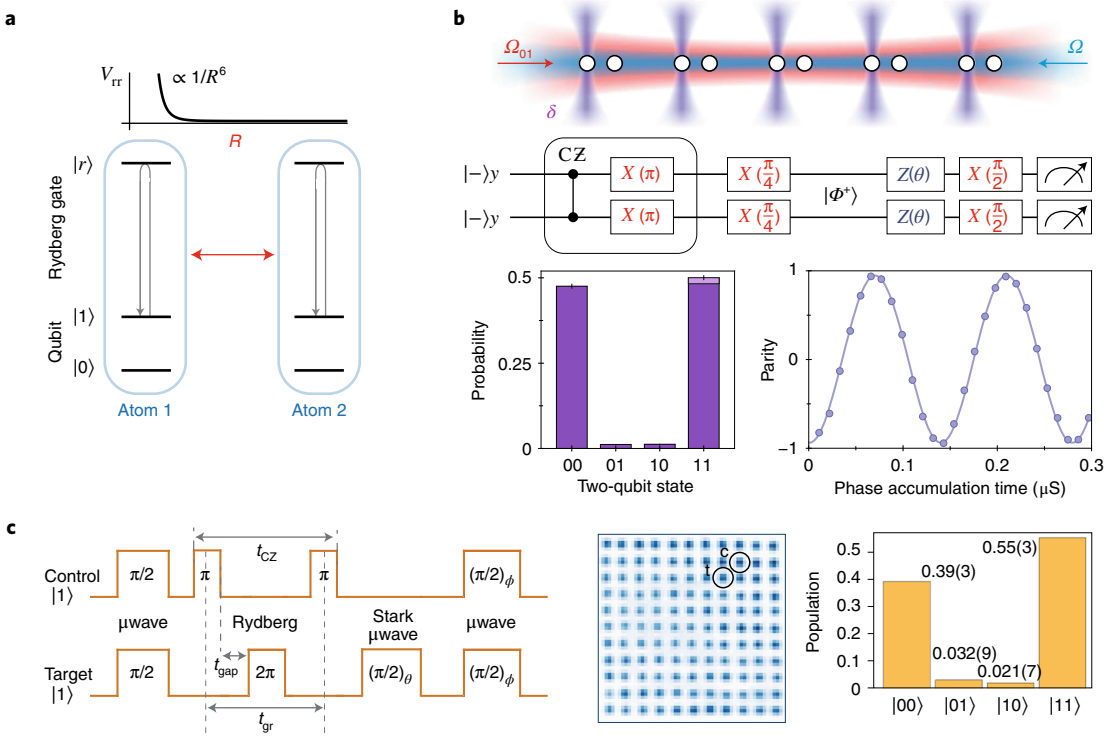

Fig. 3 | Two-qubit gates with Rydberg atoms. a, A typical system incorporates two long-lived, non-interacting levels for a qubit; in alkali atoms, the qubit is often encoded in hyperfine levels. The qubits can be arbitrarily controlled on the Bloch sphere, using resonant drives (microwave- or Raman-induced) for *X* and *Y* rotations and a.c. Stark shifts for *Z* rotations. One of the qubit states may be coupled to a high principal-quantum-number Rydberg level, so that there is a conditional phase shift depending on the two-particle spin state. Two Rydberg excited atoms a distance *R* apart, exhibit a van der Waals dipole–dipole interaction $V_{rr} = C_6/R^6$, where C_6 depends on the spectrum of Rydberg levels and dipole matrix elements. **b**, In ref. [68], a sequence of pulses on the Rydberg transition, applied globally, realize a two-qubit CZ gate on separated pairs of atoms (top). The resulting Bell state is read out with parity oscillations (bottom right) using global *Z* and *X* rotations. The oscillation contrast encodes the off-diagonal coherence of the two-particle density matrix, which, along with the measured populations in the qubit basis (bottom left), yield a final Bell-state fidelity of 97.4(3)%. Error bars are the standard error in the measurement **c**, In ref. [69], two-qubit gates are implemented with site-resolved control of the Rydberg transition in a two-dimensional array (middle; control and target atoms 'c' and 't' undergo the gate) via the π–2π–π scheme[19]. Using this gate protocol based in the local control (left) yields a Bell state that similarly may be analysed with parity rotations and population measurements. In this locally interrogated array, the two-qubit Bell-state fidelity is 88(2)% between atoms labelled c and t. Panel **b** reproduced with permission adapted from ref. [68], APS. Panel **c** adapted with permission from ref. [69], APS.

electrons, these atoms exhibit a range of optical transitions with natural linewidths ranging from tens of megahertz down to ten kilohertz and even millihertz. While the fast megahertz transition can be used for traditional laser cooling and fluorescence detection, the kilohertz-wide transitions have been the basis of new cooling schemes based on Sisyphus cooling or resolved-sideband cooling[78–80], which rely on the transition linewidth and trap frequency being on comparable timescales, a condition that is harder to achieve in alkalis. Combining the cooling performance with fast fluorescence detection has yielded high-fidelity single-atom detection with applications in quantum metrology and quantum information[25,81,82].

The ultranarrow transitions in alkaline-earth atoms—the so-called clock transitions—have been studied for over a decade for their use in high-precision time and frequency metrology[83–85]. Viewed as an oscillator, these long-lived transitions represent some of the highest-quality-factor objects in nature[27,86–88]. Using tweezers for optical atomic clocks is one direction under pursuit, as tweezers combine several strengths of trapped ions and optical lattice clocks—the two leading optical clock platforms. 'Tweezer clocks' possess the atomic isolation and high repetition rate of single-ion clocks[89–92], while being scalable to much larger atom numbers closer to those of optical lattice clocks[84,85]. The first demonstrations reached atom–laser coherence times of three seconds, approaching the state of the art, with stabilities within an order of magnitude of lattice clock records[25,87,93], as well as the capacity of the system to operate with atom numbers of 40 particles[26]. Very recent work has pushed this technique to 160 particles while maintaining atomic coherence, demonstrating precision in self-comparisons on par with the state of the art as well as reaching atomic coherence times at the half-minute scale for optical frequencies[27,87,94].

For Rydberg physics, alkaline-earth atoms also offer a number of appealing properties. By virtue of being a two-electron atom, an alkaline-earth atom with an electron in a Rydberg level retains a core resembling an alkali-like ion[95–98]. Correspondingly, a Rydberg alkaline-earth atom can be optically trapped using the polarizability of the core[99] or exhibit reduced light-shift effects[82]. Both can lead to improvements in overall two-qubit gate performance, as anti-trapping and large light shifts of Rydberg atoms present challenges in spectroscopy, necessitating flashing of the traps and consequently reduced usable interrogation times. In the context of Rydberg physics, another avenue of interest relies on the use of the long-lived excited clock state ($^3P_0$): from this level, in bosonic isotopes with zero nuclear spin, one can optically excite to a triplet series with magnetic field insensitive levels and do so with high Rabi frequency. Exploring this Rydberg spectroscopy scheme has led to recent demonstrations of record high-fidelity Rydberg spectroscopy and entanglement purity for ground-Rydberg qubits in tweezers[82].

There remain many untapped capabilities of alkaline-earth atoms. One direction of interest is to combine the tweezer clock with high-fidelity Rydberg interactions to engineer entangled states

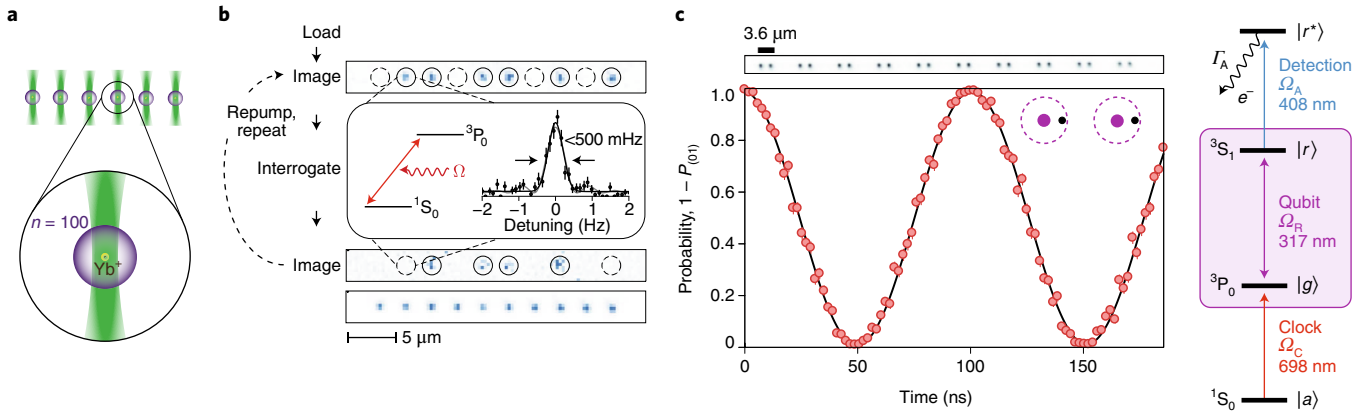

Fig. 4 | Experiments with alkaline-earth atoms in tweezers. a, Alkaline-earth and alkaline-earth-like atoms (for example, Sr and Yb, respectively) have two valence electrons. Consequently, when one electron is excited to a high-lying Rydberg level, the remaining core resembles that of alkali-like ions, which can be used for tweezer trapping of singe alkaline-earth Rydberg atoms[95,96,99]. **b**, Another application of tweezer-trapped alkaline-earth atoms is so-called tweezer clocks. Using high repetition rates, low-loss imaging and long coherence times, this new clock platform has demonstrated competitive performance with state-of-the-art systems, and could be used to create entangled clocks by leveraging the control offered by tweezer-based spin models[25–27]. **c**, Using the long-lived metastable state as a ground state, alkaline-earth atoms have been used to implement record high-fidelity Rydberg Rabi oscillations and associated entanglement between pairs of atoms (fluorescence images of which are shown). The contrast of Rydberg-blockaded Rabi oscillations is used to infer the high degree of state purity maintained during the Rydberg entangling dynamics[82]. The quality of these Rydberg measurements was enhanced by the use of high-fidelity fluorescence detection[81] and photoionization using the alkaline-earth atomic structure (right). Panels adapted with permission from: **a**, ref. [99], courtesy of Jeff Thompson; **b**, ref. [25], AAAS; **c**, ref. [82], Springer Nature Ltd.

useful for metrology[100,101]. Such entangled states can be used to improve the quantum projection noise that fundamentally limits clock performance for classical states[102]. Along a similar vein, the clock transition could be exploited as a qubit for quantum information processing. Finally, so far, the fermionic isotopes with nuclear spin have not been exploited. Doing so would allow use of the nuclear spin degree of freedom to store quantum information—a low-energy qubit that is well-isolated and easy to manipulate—while using the clock transition for shelving, enhanced measurement techniques and new gate schemes based on nuclear–electronic spin exchange[103,104]. Further, such an approach could be straightforwardly merge with established two-qubit Rydberg gates schemes for quantum information processing, exploiting the high-fidelity operations so far demonstrated with the platform.

Molecules in tweezers

As described in the previous section, alkaline-earth atoms have established new scientific directions via their increased complexity. Polar molecules, which contain two or more atoms, have even more quantum degrees of freedom plus intrinsic tunable dipolar interactions. Leveraging these intrinsic properties of molecules opens new scientific directions for fundamental physics and chemistry as well as quantum technology. Already, in the area of precision measurements, searches for an electron electric dipole moment with molecules have set the most stringent constraint by two orders of magnitude over the previous best measurement using atoms and probed a mass scale that is higher than the collision energy at the Large Hadron Collider[105]. A similar performance gain is anticipated when polar molecules are tailored for quantum science applications[106–109]. For example, several proposals outline pathways to fault-tolerant quantum logic gates by leveraging different molecular degrees of freedom for information storage and entangling operations separately, providing a way to fulfil many requirements (sometimes competing) within one coherent system[110–112]. Motivated by these prospects, many advances in quantum control of molecules have been made in the past 15 years[113–119], including demonstrations of spin coherence times on the one-second scale[120,121] and rotation[122,123] and vibration[124] coherence times on the ten-millisecond timescale.

To fully realize the potential of molecular systems for quantum sciences, full quantum state control with individual particle manipulation and readout in a low-entropy gas or array is a prerequisite and a long-standing goal. The bottom-up approach of assembling atom arrays with optical tweezers has inspired a new generation of molecular experiments. As the traditional way to obtain ultracold molecular gases relies on balancing favourable collision properties of atoms and molecules, removing such a constraint by isolating individual particles from the outset would allow higher-efficiency production of trapped molecules. Furthermore, with fewer but more highly controlled particles, the tweezer platform offers technical shortcuts that allow single-particle control of molecules[8,9,55], realizing single molecules in the internal and motional quantum ground states[10], reaching a pair density sufficient to study molecular collisions[35], and extending rotation coherence time by tenfold to a hundred milliseconds[125]. Below, we review these recent demonstrations based on two complementary approaches (Fig. 5) to obtain single molecules in optical tweezers.

Loading single molecules from a laser-cooled ensemble. Laser cooling of atoms is the starting point of all the experiments discussed before this section in this Review. However, the additions of molecular degrees of freedom—vibration and rotation—make photon cycling challenging. The recognition of molecules with diagonal Franck–Condon factors (that is, vibration wavefunction overlap of the ground and the electronic excited states is close to 1) that would allow efficient optical cycling[126,127] has motivated rapid experimental advances in laser cooling and sub-Doppler cooling of molecules[116,128–131]. To grab single molecules in tweezers (with an effective density of $10^{11}\,\mathrm{cm}^{-3}$) from a laser-cooled ensemble, an optical dipole trap with large volume and high restoring force is used as an intermediate step to enhance the ensemble density from a molecular magneto-optical trap (typical density of 10^{5}–$10^{6}\,\mathrm{cm}^{-3}$). Remarkably, this method also provides the ability to scatter a large number of photons for imaging and to induce light-assisted collisions for parity projections. Specifically, Λ-imaging demonstrated with CaF molecules can scatter thousands of photons in the presence of a tweezer trap, which allows imaging of single particles with

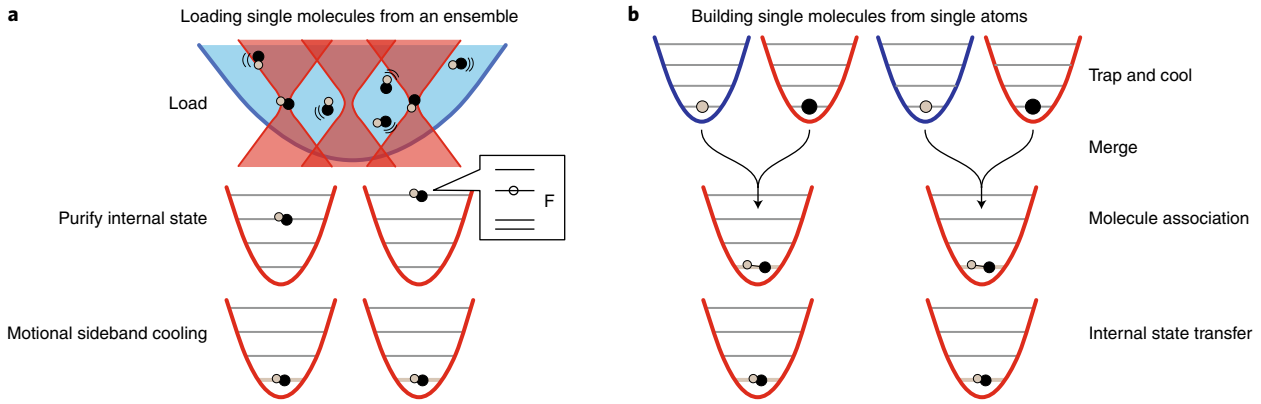

Fig. 5 | Two approaches to fully controlled single molecules in tweezers. a, One approach is to directly load single molecules from a laser-cooled ensemble and purify their internal states, as has been demonstrated in CaF[9,35], and then further cool their motional states. **b**, Another approach to single molecules is by associating single atoms and mapping all quantum control from the atoms to the resulting molecules. Once single molecules are formed, their internal state is further manipulated to bring the molecules to their vibrational ground state where they possess an appreciable dipole moment. All of the steps have been achieved in diatomic NaCs molecules[10]. With the success of these approaches, harnessing coherent molecular degrees of freedom and intrinsic dipolar interactions of fully controlled diverse molecular species for quantum science applications is underway.

a fidelity exceeding 92% currently[9]. The resulting single molecules in the tweezers are typically at a temperature of 40 μK. Empirically, light-assisted collisions of molecules in tweezers has been measured to be faster than molecular collisions in the absence of light, and ensures that traps with more than one molecule are ejected pair-wise and leave behind one or zero molecules.

As the photon-cycling schemes generally connect several Zeeman sublevels, optical pumping and microwave drives are used to further purify molecules in a chosen internal quantum state[35,132]. To reach even lower temperatures in tweezers to allow dipolar interactions to dominate over kinetic energy, motional sideband cooling methods that overcome realistic but complex molecular structure have been proposed[133] and will bring these single molecules under motional control. The ability to cycle a large numbers of photons with molecules is the key to the success of this single-molecule approach because it allows techniques developed for atoms to be realized with molecules. Higher-fidelity state preparation and detection can be straightforwardly achieved with tighter traps and larger photon collection efficiency. In addition, the same techniques can be applied to other laser-coolable species, including asymmetric-top molecules[134], which would unlock more features of neutral particles for quantum engineering[135–137].

Building single molecules from single atoms. Rather than starting with a cold gas of molecules and grabbing individual molecules out of it, one can also start with individual atoms and bring them together to make molecules. The advantage of this approach is that full control of both the internal and motional degrees of freedom of the molecules is obtained by construction in the building process. Namely, only pairs of atoms in a specific internal and motional state can be converted into molecules. One challenge to achieving this lies in simultaneous quantum control of different species of single atoms[138,139], which requires new twists to well-established atomic cooling and trapping techniques to allow their application to a wider range of species[140,141]. Another challenge is efficient molecular association, overcoming the small wavefunction overlap ($<10^{-4}$) between two atoms and a molecule. The solution is to apply a two-step approach[113–115] that has successful in producing bi-alkali molecules in bulk gases and in optical lattices to single molecules in tweezers.

The first step pairs ground-state cooled atoms into a single, albeit high-lying, vibrational quantum state via a Fano–Feshbach scattering resonance with a majority population in the motional ground state[54,55]. The second step uses a two-photon coherent process to transfer the single Feshbach molecules to the lowest vibrational state in which the molecules possess a large dipole moment that is crucial for realizing dipolar interactions. This step was recently achieved with NaCs molecules[10], which constitutes the first time that an individually controlled rovibrational ground-state molecule is predominately in its motional ground state. In addition, other molecular association methods without using Fano–Feshbach resonances are being developed, such as coherent optical Raman transfer[142], which could allow a wider range of molecular species including larger molecules to be assembled atom by atom.

Collisions. Optical tweezers provide exquisite control to study collisions with the exact collision partners prepared and the outcomes measured[8,32–34]. These parameters play an important role in the formation and the reaction of molecules. For chemical reactions to take place, a collision between molecules is the usual starting point. However, to study such a process in the ultracold regime, a sufficiently high molecular density[143] and direct probing tools are needed[144]. By inserting two laser-cooled molecules in a tweezer, a pair density many orders of magnitude higher than the initial laser-cooled gas is achieved and processes involving three particles are eliminated, allowing the observation of collisions of exactly two CaF molecules[35] with a loss rate close to the universal rate that has also been widely observed in collisions of bi-alkali molecules. Furthermore, such a platform has recently served as a testbed to demonstrate microwave shielding of collisions[145]. In the near future, optical tweezers offer a promising and clean platform to probe few-body physics with complex interactions, such as atom–molecule and molecule–molecule.

The introduction of tweezers to molecular systems in the past five to seven years has fulfilled the long-standing aim to bring individual molecules under full quantum control. Immediate goals on the horizon are to scale up the number of single molecules using optical engineering techniques that have been demonstrated with atom arrays and to exploit complex molecular degrees of freedom and their intrinsic dipolar interactions for exciting applications such as quantum simulations of spin models[107,108] and synthetic dimensions for Hamiltonian engineering[146], realizing chiral spin liquids[147] and entangling logic gates[106,110,112]. Furthermore, with the rapid recent progress aided by optical tweezers, we can expect diverse molecular species tailored for different quantum science applications to become available in the near future.

Future directions

Controllable arrays of single neutral atoms in tweezers have proven to be a powerful platform, impacting an impressive range of subfields within quantum science, including information processing[2,3,7,24,68,69,75,82], many-body physics[6,20–24], metrology[25,26], quantum optics[17,18], quantum networks[28] and ultracold chemistry[8,33,35]. Yet, all indications are that we are only at the early stages of developing this platform. Technical improvements in control, gate fidelities and scalability occur on a yearly basis; meanwhile, a growing industry sector—including companies such as QuEra Computing, Cold Quanta and Atom Computing—for Rydberg-based quantum computing is likely to begin making its own contributions. Nascent platforms with new particles, such as alkaline-earths and molecules, are establishing many different research directions. One can be optimistic that the future is bright for this emerging player in the quantum science arena.

Received: 5 September 2020; Accepted: 4 August 2021;
Published online: 11 November 2021

References

1. Schlosser, N., Reymond, G., Protsenko, I. & Grangier, P. Sub-Poissonian loading of single atoms in a microscopic dipole trap. *Nature* **411**, 1024–1027 (2001).
2. Wilk, T. et al. Entanglement of two individual neutral atoms using Rydberg blockade. *Phys. Rev. Lett.* **104**, 010502 (2010).
3. Isenhower, L. et al. Demonstration of a neutral atom controlled-NOT quantum gate. *Phys. Rev. Lett.* **104**, 010503 (2010).
4. Kaufman, A. M. et al. Two-particle quantum interference in tunnel-coupled optical tweezers. *Science* **345**, 306–309 (2014).
5. Xia, T. et al. Randomized benchmarking of single-qubit gates in a 2D array of neutral-atom qubits. *Phys. Rev. Lett.* **114**, 100503 (2015).
6. Bernien, H. et al. Probing many-body dynamics on a 51-atom quantum simulator. *Nature* **551**, 579–584 (2017).
7. Levine, H. et al. High-fidelity control and entanglement of Rydberg-atom qubits. *Phys. Rev. Lett.* **121**, 123603 (2018).
8. Liu, L. R. et al. Building one molecule from a reservoir of two atoms. *Science* **360**, 900–903 (2018).
9. Anderegg, L. et al. An optical tweezer array of ultracold molecules. *Science* **365**, 1156–1158 (2019).
10. Cairncross, W. B. et al. Assembly of a rovibrational ground state molecule in an optical tweezer. *Phys. Rev. Lett.* **126**, 123402 (2021).
11. Miroshnychenko, Y. et al. An atom-sorting machine. *Nature* **442**, 151 (2006).
12. Barredo, D., de Léséleuc, S., Lienhard, V., Lahaye, T. & Browaeys, A. An atom-by-atom assembler of defect-free arbitrary 2D atomic arrays. *Science* **354**, 1021–1023 (2016).
13. Endres, M. et al. Atom-by-atom assembly of defect-free one-dimensional cold atom arrays. *Science* **354**, 1024–1027 (2016).
14. Robens, C. et al. Low-entropy states of neutral atoms in polarization-synthesized optical lattices. *Phys. Rev. Lett.* **118**, 065302 (2017).
15. Kumar, A., Wu, T.-Y., Giraldo, F. & Weiss, D. S. Sorting ultracold atoms in a three-dimensional optical lattice in a realization of Maxwell's demon. *Nature* **561**, 83–87 (2018).
16. Bloch, I., Dalibard, J. & Zwerger, W. Many-body physics with ultracold gases. *Rev. Mod. Phys.* **80**, 885–964 (2008).
17. Darquié, B. et al. Controlled single-photon emission from a single trapped two-level atom. *Science* **309**, 454–456 (2005).
18. Beugnon, J. et al. Quantum interference between two single photons emitted by independently trapped atoms. *Nature* **440**, 779–782 (2006).
19. Saffman, M., Walker, T. G. & Molmer, K. Quantum information with Rydberg atoms. *Rev. Mod. Phys.* **82**, 2313–2363 (2010).
20. Lienhard, V. et al. Observing the space- and time-dependent growth of correlations in dynamically tuned synthetic ising models with antiferromagnetic interactions. *Phys. Rev. X* **8**, 021070 (2018).
21. Keesling, A. et al. Quantum Kibble–Zurek mechanism and critical dynamics on a programmable Rydberg simulator. *Nature* **568**, 207–211 (2019).
22. Omran, A. et al. Generation and manipulation of Schrödinger cat states in Rydberg atom arrays. *Science* **365**, 570–574 (2019).
23. de Léséleuc, S. et al. Observation of a symmetry-protected topological phase of interacting bosons with Rydberg atoms. *Science* **365**, 775–780 (2019).
24. Browaeys, A. & Lahaye, T. Many-body physics with individually controlled Rydberg atoms. *Nat. Phys.* **16**, 132–142 (2020).
25. Norcia, M. A. et al. Seconds-scale coherence on an optical clock transition in a tweezer array. *Science* **366**, 93–97 (2019).
26. Madjarov, I. S. et al. An atomic-array optical clock with single-atom readout. *Phys. Rev. X* **9**, 041052 (2019).
27. Young, A. W. et al. Half-minute-scale atomic coherence and high relative stability in a tweezer clock. *Nature* **588**, 408–413 (2020).
28. Thompson, J. D. et al. Coupling a single trapped atom to a nanoscale optical cavity. *Science* **340**, 1202–1205 (2013).
29. Kim, M. E., Chang, T.-H., Fields, B. M., Chen, C.-A. & Hung, C.-L. Trapping single atoms on a nanophotonic circuit with configurable tweezer lattices. *Nat. Commun.* **10**, 1647 (2019).
30. Nayak, K. P., Wang, J. & Keloth, J. Real-time observation of single atoms trapped and interfaced to a nanofiber cavity. *Phys. Rev. Lett.* **123**, 213602 (2019).
31. Béguin, J.-B. et al. Advanced apparatus for the integration of nanophotonics and cold atoms. *Optica* **7**, 1–2 (2020).
32. Xu, P. et al. Interaction-induced decay of a heteronuclear two-atom system. *Nat. Commun.* **6**, 7803 (2015).
33. Reynolds, L. A. et al. Direct measurements of collisional dynamics in cold atom triads. *Phys. Rev. Lett.* **124**, 073401 (2020).
34. Hood, J. D. et al. Multichannel interactions of two atoms in an optical tweezer. *Phys. Rev. Res.* **2**, 023108 (2020).
35. Cheuk, L. W. et al. Observation of collisions between two ultracold ground-state caf molecules. *Phys. Rev. Lett.* **125**, 043401 (2020).
36. Schlosser, N., Reymond, G. & Grangier, P. Collisional blockade in microscopic optical dipole traps. *Phys. Rev. Lett.* **89**, 023005 (2002).
37. Jones, M. P. A. et al. Fast quantum state control of a single trapped neutral atom. *Phys. Rev. A* **75**, 040301 (2007).
38. Beugnon, J. et al. Two-dimensional transport and transfer of a single atomic qubit in optical tweezers. *Nat. Phys.* **3**, 696–699 (2007).
39. Kaufman, A. M. et al. Entangling two transportable neutral atoms via local spin exchange. *Nature* **527**, 208–211 (2015).
40. Weiss, D. S. et al. Another way to approach zero entropy for a finite system of atoms. *Phys. Rev. A* **70**, 040302 (2004).
41. Serwane, F. et al. Deterministic preparation of a tunable few-fermion system. *Science* **332**, 336–338 (2011).
42. Wenz, A. N. et al. From few to many: observing the formation of a Fermi sea one atom at a time. *Science* **342**, 457–460 (2013).
43. Zürn, G. et al. Fermionization of two distinguishable fermions. *Phys. Rev. Lett.* **108**, 075303 (2012).
44. Murmann, S. et al. Two fermions in a double well: exploring a fundamental building block of the Hubbard model. *Phys. Rev. Lett.* **114**, 080402 (2015).
45. Preiss, P. M. et al. High-contrast interference of ultracold fermions. *Phys. Rev. Lett.* **122**, 143602 (2019).
46. Bergschneider, A. et al. Experimental characterization of two-particle entanglement through position and momentum correlations. *Nat. Phys.* **15**, 640–644 (2019).
47. Becher, J. H. et al. Measurement of identical particle entanglement and the influence of antisymmetrization. *Phys. Rev. Lett.* **125**, 180402 (2020).
48. Bayha, L. et al. Observing the emergence of a quantum phase transition shell by shell. *Nature* **587**, 583–587 (2020).
49. Holten, M. et al. Observation of Pauli crystals. *Phys. Rev. Lett.* **126**, 020401 (2021).
50. Kaufman, A. M., Lester, B. J. & Regal, C. A. Cooling a single atom in an optical tweezer to its quantum ground state. *Phys. Rev. X* **2**, 041014 (2012).
51. Thompson, J. D., Tiecke, T. G., Zibrov, A. S., Vuletić, V. & Lukin, M. D. Coherence and Raman sideband cooling of a single atom in an optical tweezer. *Phys. Rev. Lett.* **110**, 133001 (2013).
52. Diedrich, F., Bergquist, J. C., Itano, W. M. & Wineland, D. J. Laser cooling to the zero-point energy of motion. *Phys. Rev. Lett.* **62**, 403–406 (1989).
53. Monroe, C. et al. Resolved-sideband Raman cooling of a bound atom to the 3D zero-point energy. *Phys. Rev. Lett.* **75**, 4011–4014 (1995).
54. Zhang, J. T. et al. Forming a single molecule by magnetoassociation in an optical tweezer. *Phys. Rev. Lett.* **124**, 253401 (2020).
55. He, X. et al. Coherently forming a single molecule in an optical trap. *Science* **370**, 331–335 (2020).
56. Barredo, D., Lienhard, V., de Léséleuc, S., Lahaye, T. & Browaeys, A. Synthetic three-dimensional atomic structures assembled atom by atom. *Nature* **561**, 79–82 (2018).
57. Ebadi, S. et al. Quantum phases of matter on a 256-atom programmable quantum simulator. *Nature* **595**, 227–232 (2021).
58. Scholl, P. et al. Quantum simulation of 2D antiferromagnets with hundreds of Rydberg atoms. *Nature* **595**, 233–238 (2021).
59. Grünzweig, T., Hilliard, A., McGovern, M. & Andersen, M. Near-deterministic preparation of a single atom in an optical microtrap. *Nat. Phys.* **6**, 951–954 (2010).
60. Lester, B. J., Luick, N., Kaufman, A. M., Reynolds, C. M. & Regal, C. A. Rapid production of uniformly filled arrays of neutral atoms. *Phys. Rev. Lett.* **115**, 073003 (2015).
61. Brown, M. O., Thiele, T., Kiehl, C., Hsu, T.-W. & Regal, C. A. Gray-molasses optical-tweezer loading: controlling collisions for scaling atom-array assembly. *Phys. Rev. X* **9**, 011057 (2019).

62. Jaksch, D. et al. Fast quantum gates for neutral atoms. *Phys. Rev. Lett.* **85**, 2208–2211 (2000).
63. Brennen, G. K., Deutsch, I. H. & Jessen, P. S. Entangling dipole–dipole interactions for quantum logic with neutral atoms. *Phys. Rev. A* **61**, 062309 (2000).
64. Urban, E. et al. Observation of Rydberg blockade between two atoms. *Nat. Phys.* **5**, 110–114 (2009).
65. Gaëtan, A. et al. Observation of collective excitation of two individual atoms in the Rydberg blockade regime. *Nat. Phys.* **5**, 115–118 (2009).
66. Jau, Y. Y., Hankin, A. M., Keating, T., Deutsch, I. H. & Biedermann, G. W. Entangling atomic spins with a Rydberg-dressed spin-flip blockade. *Nat. Phys.* **12**, 71–74 (2016).
67. de Léséleuc, S., Barredo, D., Lienhard, V., Browaeys, A. & Lahaye, T. Analysis of imperfections in the coherent optical excitation of single atoms to rydberg states. *Phys. Rev. A* **97**, 053803 (2018).
68. Levine, H. et al. Parallel implementation of high-fidelity multiqubit gates with neutral atoms. *Phys. Rev. Lett.* **123**, 170503 (2019).
69. Graham, T. M. et al. Rydberg-mediated entanglement in a two-dimensional neutral atom qubit array. *Phys. Rev. Lett.* **123**, 230501 (2019).
70. Saffman, M. & Mølmer, K. Efficient multiparticle entanglement via asymmetric Rydberg blockade. *Phys. Rev. Lett.* **102**, 240502 (2009).
71. de Léséleuc, S., Barredo, D., Lienhard, V., Browaeys, A. & Lahaye, T. Optical control of the resonant dipole–dipole interaction between Rydberg atoms. *Phys. Rev. Lett.* **119**, 053202 (2017).
72. Pichler, H., Wang, S., Zhou, L., Choi, S. & Lukin, M. Quantum optimization for maximum independent set using Rydberg atom arrays. Preprint at https://arxiv.org/abs/1808.10816 (2018).
73. Zhou, L., Wang, S.-T., Choi, S., Pichler, H. & Lukin, M. D. Quantum approximate optimization algorithm: performance, mechanism, and implementation on near-term devices. *Phys. Rev. X* **10**, 021067 (2020).
74. Wild, D. S., Sels, D., Pichler, H., Zanoci, C. & Lukin, M. Quantum sampling algorithms for near-term devices. *Phys. Rev. Lett.* **127**, 100504 (2020).
75. Saffman, M. Quantum computing with atomic qubits and Rydberg interactions: progress and challenges. *J. Phys. B* **49**, 202001 (2016).
76. Cortiñas, R. G. et al. Laser trapping of circular Rydberg atoms. *Phys. Rev. Lett.* **124**, 123201 (2020).
77. Beterov, I. I. & Saffman, M. Rydberg blockade, förster resonances, and quantum state measurements with different atomic species. *Phys. Rev. A* **92**, 042710 (2015).
78. Norcia, M. A., Young, A. W. & Kaufman, A. M. Microscopic control and detection of ultracold strontium in optical-tweezer arrays. *Phys. Rev. X* **8**, 041054 (2018).
79. Cooper, A. et al. Alkaline-earth atoms in optical tweezers. *Phys. Rev. X* **8**, 041055 (2018).
80. Saskin, S., Wilson, J. T., Grinkemeyer, B. & Thompson, J. D. Narrow-line cooling and imaging of ytterbium atoms in an optical tweezer array. *Phys. Rev. Lett.* **122**, 143002 (2019).
81. Covey, J. P., Madjarov, I. S., Cooper, A. & Endres, M. 2000-times repeated imaging of strontium atoms in clock-magic tweezer arrays. *Phys. Rev. Lett.* **122**, 173201 (2019).
82. Madjarov, I. S. et al. High-fidelity entanglement and detection of alkaline-earth Rydberg atoms. *Nat. Phys.* **16**, 857–861 (2020).
83. Ludlow, A. D., Boyd, M. M., Ye, J., Peik, E. & Schmidt, P. O. Optical atomic clocks. *Rev. Mod. Phys.* **87**, 637–701 (2015).
84. Bloom, B. J. et al. An optical lattice clock with accuracy and stability at the 10^{-18} level. *Nature* **506**, 71–75 (2014).
85. McGrew, W. F. et al. Atomic clock performance enabling geodesy below the centimetre level. *Nature* **564**, 87–90 (2018).
86. Hume, D. B. & Leibrandt, D. R. Probing beyond the laser coherence time in optical clock comparisons. *Phys. Rev. A* **93**, 032138 (2016).
87. Campbell, S. L. et al. A Fermi-degenerate three-dimensional optical lattice clock. *Science* **358**, 90–94 (2017).
88. Clements, E. R. et al. Lifetime-limited interrogation of two independent $^{27}Al^+$ clocks using correlation spectroscopy. *Phys. Rev. Lett.* **125**, 243602 (2020).
89. Diddams, S. A. et al. An optical clock based on a single trapped $^{199}Hg^+$ ion. *Science* **293**, 825–828 (2001).
90. Chou, C. W., Hume, D. B., Koelemeij, J. C. J., Wineland, D. J. & Rosenband, T. Frequency comparison of two high-accuracy Al^+ optical clocks. *Phys. Rev. Lett.* **104**, 070802 (2010).
91. Chou, C. W., Hume, D. B., Thorpe, M. J., Wineland, D. J. & Rosenband, T. Quantum coherence between two atoms beyond $Q=10^{15}$. *Phys. Rev. Lett.* **106**, 160801 (2011).
92. Brewer, S. M. et al. $^{27}Al^+$ quantum-logic clock with a systematic uncertainty below 10^{-18}. *Phys. Rev. Lett.* **123**, 033201 (2019).
93. Oelker, E. et al. Demonstration of 4.8×10^{-17} stability at 1 s for two independent optical clocks. *Nat. Photon.* **13**, 714–719 (2019).
94. Marti, G. E. et al. Imaging optical frequencies with 100μHz precision and 1.1μm resolution. *Phys. Rev. Lett.* **120**, 103201 (2018).
95. Mukherjee, R., Millen, J., Nath, R., Jones, M. P. A. & Pohl, T. Many-body physics with alkaline-earth Rydberg lattices. *J. Phys. B* **44**, 184010 (2011).
96. Topcu, T. & Derevianko, A. Divalent Rydberg atoms in optical lattices: intensity landscape and magic trapping. *Phys. Rev. A* **89**, 023411 (2014).
97. Topcu, T. & Derevianko, A. Possibility of triple magic trapping of clock and Rydberg states of divalent atoms in optical lattices. *J. Phys. B* **49**, 144004 (2016).
98. Robicheaux, F., Booth, D. W. & Saffman, M. Theory of long-range interactions for Rydberg states attached to hyperfine-split cores. *Phys. Rev. A* **97**, 022508 (2018).
99. Wilson, J. et al. Trapped arrays of alkaline earth Rydberg atoms in optical tweezers. Preprint at https://arxiv.org/abs/1912.08754 (2019).
100. Gil, L. I. R., Mukherjee, R., Bridge, E. M., Jones, M. P. A. & Pohl, T. Spin squeezing in a Rydberg lattice clock. *Phys. Rev. Lett.* **112**, 103601 (2014).
101. Kaubruegger, R. et al. Variational spin-squeezing algorithms on programmable quantum sensors. *Phys. Rev. Lett.* **123**, 260505 (2019).
102. Wineland, D. J., Bollinger, J. J., Itano, W. M., Moore, F. L. & Heinzen, D. J. Spin squeezing and reduced quantum noise in spectroscopy. *Phys. Rev. A* **46**, R6797–R6800 (1992).
103. Cappellini, G. et al. Direct observation of coherent interorbital spin-exchange dynamics. *Phys. Rev. Lett.* **113**, 120402 (2014).
104. Pagano, G., Scazza, F. & Foss-Feig, M. Fast and scalable quantum information processing with two-electron atoms in optical tweezer arrays. *Adv. Quantum Technol.* **2**, 1800067 (2019).
105. Andreev, V. et al. Improved limit on the electric dipole moment of the electron. *Nature* **562**, 355–360 (2018).
106. DeMille, D. Quantum computation with trapped polar molecules. *Phys. Rev. Lett.* **88**, 067901 (2002).
107. Micheli, A., Brennen, G. & Zoller, P. A toolbox for lattice-spin models with polar molecules. *Nat. Phys.* **2**, 341–347 (2006).
108. Gorshkov, A. V. et al. Tunable superfluidity and quantum magnetism with ultracold polar molecules. *Phys. Rev. Lett.* **107**, 115301 (2011).
109. Yan, B. et al. Observation of dipolar spin-exchange interactions with lattice-confined polar molecules. *Nature* **501**, 521–525 (2013).
110. Ni, K.-K., Rosenband, T. & Grimes, D. D. Dipolar exchange quantum logic gate with polar molecules. *Chem. Sci.* **9**, 6830–6838 (2018).
111. Hudson, E. R. & Campbell, W. C. Dipolar quantum logic for freely rotating trapped molecular ions. *Phys. Rev. A* **98**, 040302 (2018).
112. Hughes, M. et al. Robust entangling gate for polar molecules using magnetic and microwave fields. *Phys. Rev. A* **101**, 062308 (2020).
113. Danzl, J. G. et al. Quantum gas of deeply bound ground state molecules. *Science* **321**, 1062–1066 (2008).
114. Ni, K.-K. et al. A high phase-space-density gas of polar molecules. *Science* **322**, 231–235 (2008).
115. Lang, F., Winkler, K., Strauss, C., Grimm, R. & Denschlag, J. H. Ultracold triplet molecules in the rovibrational ground state. *Phys. Rev. Lett.* **101**, 133005 (2008).
116. Shuman, E. S., Barry, J. F. & DeMille, D. Laser cooling of a diatomic molecule. *Nature* **467**, 820–823 (2010).
117. Prehn, A., Ibrügger, M., Glöckner, R., Rempe, G. & Zeppenfeld, M. Optoelectrical cooling of polar molecules to submillikelvin temperatures. *Phys. Rev. Lett.* **116**, 063005 (2016).
118. Chou, C.-W. et al. Preparation and coherent manipulation of pure quantum states of a single molecular ion. *Nature* **545**, 203–207 (2017).
119. De Marco, L. et al. A degenerate Fermi gas of polar molecules. *Science* **363**, 853–856 (2019).
120. Park, J. W., Yan, Z. Z., Loh, H., Will, S. A. & Zwierlein, M. W. Second-scale nuclear spin coherence time of ultracold $^{23}Na^{40}K$ molecules. *Science* **357**, 372–375 (2017).
121. Gregory, P. D., Blackmore, J. A., Bromley, S. L., Hutson, J. M. & Cornish, S. L. Robust storage qubits in ultracold polar molecules. *Nat. Phys.* **17**, 1149–1153 (2021).
122. Seeßelberg, F. et al. Extending rotational coherence of interacting polar molecules in a spin-decoupled magic trap. *Phys. Rev. Lett.* **121**, 253401 (2018).
123. Caldwell, L. et al. Long rotational coherence times of molecules in a magnetic trap. *Phys. Rev. Lett.* **124**, 063001 (2020).
124. Kondov, S. S. et al. Molecular lattice clock with long vibrational coherence. *Nat. Phys.* **15**, 1118–1122 (2019).
125. Burchesky, S. et al. Rotational coherence times of polar molecules in optical tweezers. Preprint at https://arxiv.org/abs/2105.15199 (2021).
126. Di Rosa, M. D. Laser-cooling molecules—concept, candidates, and supporting hyperfine-resolved measurements of rotational lines in the A–X(0,0) band of CaH. *Eur. Phys. J. D* **31**, 395–402 (2004).
127. Stuhl, B. K., Sawyer, B. C., Wang, D. & Ye, J. Magneto-optical trap for polar molecules. *Phys. Rev. Lett.* **101**, 243002 (2008).
128. Barry, J. F., McCarron, D. J., Norrgard, E. B., Steinecker, M. H. & DeMille, D. Magneto-optical trapping of a diatomic molecule. *Nature* **512**, 286–289 (2014).

129. Truppe, S. et al. Molecules cooled below the doppler limit. *Nat. Phys.* **13**, 1173–1176 (2017).
130. Cheuk, L. W. et al. Λ-enhanced imaging of molecules in an optical trap. *Phys. Rev. Lett.* **121**, 083201 (2018).
131. Ding, S., Wu, Y., Finneran, I. A., Burau, J. J. & Ye, J. Sub-Doppler cooling and compressed trapping of YO molecules at μK temperatures. *Phys. Rev. X* **10**, 021049 (2020).
132. Williams, H. J. et al. Magnetic trapping and coherent control of laser-cooled molecules. *Phys. Rev. Lett.* **120**, 163201 (2018).
133. Caldwell, L. & Tarbutt, M. R. Sideband cooling of molecules in optical traps. *Phys. Rev. Res.* **2**, 013251 (2020).
134. Mitra, D. et al. Direct laser cooling of a symmetric top molecule. *Science* **369**, 1366–1369 (2020).
135. Wall, M. L., Maeda, K. & Carr, L. D. Realizing unconventional quantum magnetism with symmetric top molecules. *New J. Phys.* **17**, 025001 (2015).
136. Yu, P., Cheuk, L. W., Kozyryev, I. & Doyle, J. M. A scalable quantum computing platform using symmetric-top molecules. *New J. Phys.* **21**, 093049 (2019).
137. Kozyryev, I. & Hutzler, N. R. Precision measurement of time-reversal symmetry violation with laser-cooled polyatomic molecules. *Phys. Rev. Lett.* **119**, 133002 (2017).
138. Liu, L. R. et al. Molecular assembly of ground-state cooled single atoms. *Phys. Rev. X* **9**, 021039 (2019).
139. Wang, K. et al. Preparation of a heteronuclear two-atom system in the three-dimensional ground state in an optical tweezer. *Phys. Rev. A* **100**, 063429 (2019).
140. Hutzler, N. R., Liu, L. R., Yu, Y. & Ni, K.-K. Eliminating light shifts for single atom trapping. *New J. Phys.* **19**, 023007 (2017).
141. Yu, Y. et al. Motional-ground-state cooling outside the lamb-dicke regime. *Phys. Rev. A* **97**, 063423 (2018).
142. Yu, Y. et al. Coherent optical creation of a single molecule. Preprint at https://arxiv.org/abs/2012.09043 (2020).
143. Ospelkaus, S. et al. Controlling the hyperfine state of rovibronic ground-state polar molecules. *Phys. Rev. Lett.* **104**, 030402 (2010).
144. Hu, M.-G. et al. Direct observation of bimolecular reactions of ultracold KRb molecules. *Science* **366**, 1111–1115 (2019).
145. Anderegg, L. et al. Observation of microwave shielding of ultracold molecules. *Science* **373**, abg9502 (2021).
146. Sundar, B., Gadway, B. & Hazzard, K. R. A. Synthetic dimensions in ultracold polar molecules. *Sci. Rep.* **8**, 3422 (2018).
147. Yao, N. Y., Zaletel, M. P., Stamper-Kurn, D. M. & Vishwanath, A. A quantum dipolar spin liquid. *Nat. Phys.* **14**, 405–410 (2018).
148. Sompet, P., Carpentier, A. V., Fung, Y. H., McGovern, M. & Andersen, M. F. Dynamics of two atoms undergoing light-assisted collisions in an optical microtrap. *Phys. Rev. A* **88**, 051401 (2013).
149. Vuletić, V., Chin, C., Kerman, A. J. & Chu, S. Degenerate Raman sideband cooling of trapped cesium atoms at very high atomic densities. *Phys. Rev. Lett.* **81**, 5768–5771 (1998).
150. Han, D.-J. et al. 3D Raman sideband cooling of cesium atoms at high density. *Phys. Rev. Lett.* **85**, 724–727 (2000).

Acknowledgements

We thank W. Cairncross for assisting with the preparation of Fig. 5, and N. Schine and L. Liu for critical reading of the manuscript. A.M.K. acknowledges support from NIST. K.-K.N. acknowledges support from the AROSR (FA9550-19-1-0089).

Competing interests

The authors declare no competing interests.

Additional information

Correspondence should be addressed to Adam M. Kaufman or Kang-Kuen Ni.

Peer review information *Nature Physics* thanks the anonymous reviewers for their contribution to the peer review of this work.